Numerical Simulations of Generic Singularities

David Garfinkle*

Department of Physics, University of Guelph, Guelph, Ontario N1G 2W1, Canada
and Perimeter Institute for Theoretical Physics, 35 King Street North, Waterloo, Ontario N2J 2W9, Canada

(Received 29 December 2003; published 12 October 2004)

Numerical simulations of the approach to the singularity in vacuum spacetimes are presented here. The spacetimes examined have no symmetries and can be regarded as representing the general behavior of singularities. It is found that the singularity is spacelike and that, as it is approached, the spacetime dynamics becomes local and oscillatory.

DOI: 10.1103/PhysRevLett.93.161101 PACS numbers: 04.20.Dw, 04.25.Dm

A longstanding problem in general relativity has been to find the general behavior of singularities. Several results, both analytical [1] and numerical [2] have been obtained. However, for most of the results, the spacetimes have one or more symmetries. Only for scalar field matter have results been found when there are no symmetries. [3,4] For vacuum, Belinski, Lifschitz and Khalatnikov [5] (BKL) have conjectured that the generic singularity is local, spacelike, and oscillatory. This conjecture has been reformulated and put more precisely by Uggla *et al.*[6]

In this Letter are presented numerical simulations of the approach to the singularity in vacuum spacetimes with no symmetries. The results support the BKL conjecture.

The system evolved here is essentially that of reference [6] but specialized to the vacuum case and with a slightly different choice of gauge. Here the spacetime is described in terms of a coordinate system (t, x^i) and a tetrad $(\mathbf{e}_0, \mathbf{e}_\alpha)$ where both the spatial coordinate index i and the spatial tetrad index α go from one to 3. Choose $\mathbf{e}_0$ to be hypersurface orthogonal with the relation between tetrad and coordinates of the form $\mathbf{e}_0 = N^{-1}\partial_t$ and $\mathbf{e}_\alpha = e_\alpha{}^i\partial_i$ where N is the lapse and the shift is chosen to be zero. Choose the spatial frame $\{\mathbf{e}_\alpha\}$ to be Fermi propagated along the integral curves of $\mathbf{e}_0$. The commutators of the tetrad components are decomposed as follows:

$$[\mathbf{e}_0, \mathbf{e}_\alpha] = \dot{u}_\alpha \mathbf{e}_0 - (H\delta_\alpha{}^\beta + \sigma_\alpha{}^\beta)\mathbf{e}_\beta \tag{1}$$

and

$$[\mathbf{e}_\alpha, \mathbf{e}_\beta] = (2a_{[\alpha}\delta_{\beta]}{}^\gamma + \epsilon_{\alpha\beta\delta}n^{\delta\gamma})\mathbf{e}_\gamma \tag{2}$$

where $n^{\alpha\beta}$ is symmetric, and $\sigma^{\alpha\beta}$ is symmetric and trace-free.

Scale invariant variables are defined as follows:

$$\begin{aligned}&\{\boldsymbol{\partial}_0, \boldsymbol{\partial}_\alpha\} \equiv \{\mathbf{e}_0, \mathbf{e}_\alpha\}/H,\\ &\{E_\alpha{}^i, \Sigma_{\alpha\beta}, A^\alpha, N_{\alpha\beta}\} \equiv \{e_\alpha{}^i, \sigma_{\alpha\beta}, a^\alpha, n_{\alpha\beta}\}/H,\\ &q + 1 \equiv -\boldsymbol{\partial}_0 \ln H, \quad \text{and} \quad r_\alpha \equiv -\boldsymbol{\partial}_\alpha \ln H.\end{aligned} \tag{3}$$

Finally choose the lapse to be $N = H^{-1}$. The relation between scale invariant frame derivatives and coordinate derivatives is $\boldsymbol{\partial}_0 = \partial_t$ and $\boldsymbol{\partial}_\alpha = E_\alpha{}^i\partial_i$. From the vacuum Einstein equations one obtains the following evolution equations:

$$\partial_t E_\alpha{}^i = F_\alpha{}^\beta E_\beta{}^i, \tag{4}$$

$$\partial_t r_\alpha = F_\alpha{}^\beta r_\beta + \boldsymbol{\partial}_\alpha q, \tag{5}$$

$$\partial_t A^\alpha = F^\alpha{}_\beta A^\beta + \frac{1}{2}\boldsymbol{\partial}_\beta \Sigma^{\alpha\beta}, \tag{6}$$

$$\begin{aligned}\partial_t \Sigma^{\alpha\beta} = {}&(q-2)\Sigma^{\alpha\beta} - 2N^{\langle\alpha}{}_\gamma N^{\beta\rangle\gamma} + N_\gamma{}^\gamma N^{\langle\alpha\beta\rangle}\\ &+ \boldsymbol{\partial}^{\langle\alpha} r^{\beta\rangle} - \boldsymbol{\partial}^{\langle\alpha} A^{\beta\rangle} + 2r^{\langle\alpha} A^{\beta\rangle}\\ &+ \epsilon^{\gamma\delta\langle\alpha}(\boldsymbol{\partial}_\gamma - 2A_\gamma)N^{\beta\rangle}{}_\delta,\end{aligned} \tag{7}$$

$$\partial_t N^{\alpha\beta} = qN^{\alpha\beta} + 2\Sigma^{(\alpha}{}_\delta N^{\beta)\delta} - \epsilon^{\gamma\delta(\alpha}\boldsymbol{\partial}_\gamma \Sigma^{\beta)}{}_\delta, \tag{8}$$

and

$$\begin{aligned}\partial_t q = {}&\left[2(q-2) + \frac{1}{3}(2A^\alpha - r^\alpha)\boldsymbol{\partial}_\alpha - \frac{1}{3}\boldsymbol{\partial}^\alpha\boldsymbol{\partial}_\alpha\right]q\\ &- \frac{4}{3}\boldsymbol{\partial}_\alpha r^\alpha + \frac{8}{3}A^\alpha r_\alpha + \frac{2}{3}r_\beta\boldsymbol{\partial}_\alpha\Sigma^{\alpha\beta} - 2\Sigma^{\alpha\beta}W_{\alpha\beta}.\end{aligned} \tag{9}$$

Here angle brackets denote the symmetric trace-free part, and $F_{\alpha\beta}$ and $W_{\alpha\beta}$ are given by

$$F_{\alpha\beta} \equiv q\delta_{\alpha\beta} - \Sigma_{\alpha\beta} \tag{10}$$

and

$$\begin{aligned}W_{\alpha\beta} \equiv {}&\frac{2}{3}N_{\alpha\gamma}N_\beta{}^\gamma - \frac{1}{3}N^\gamma{}_\gamma N_{\alpha\beta} + \frac{1}{3}\boldsymbol{\partial}_\alpha A_\beta - \frac{2}{3}\boldsymbol{\partial}_\alpha r_\beta\\ &- \frac{1}{3}\epsilon^{\gamma\delta}{}_\alpha(\boldsymbol{\partial}_\gamma - 2A_\gamma)N_{\beta\delta}.\end{aligned} \tag{11}$$

In addition to the evolution equations, the variables satisfy constraint equations as follows:

$$0 = (C_{\text{com}})^i_{\alpha\beta} \equiv 2(\boldsymbol{\partial}_{[\alpha} - r_{[\alpha} - A_{[\alpha})E_{\beta]}{}^i - \epsilon_{\alpha\beta\delta}N^{\delta\gamma}E_\gamma{}^i, \tag{12}$$

$$\begin{aligned}0 = C_{\mathrm{G}} \equiv {}&1 + \frac{1}{3}(2\boldsymbol{\partial}_\alpha - 2r_\alpha - 3A_\alpha)A^\alpha - \frac{1}{6}N_{\alpha\beta}N^{\alpha\beta}\\ &+ \frac{1}{12}(N^\alpha{}_\alpha)^2 - \frac{1}{6}\Sigma_{\alpha\beta}\Sigma^{\alpha\beta},\end{aligned} \tag{13}$$

$$0 = (C_C)^\alpha \equiv \boldsymbol{\partial}_\beta \Sigma^{\alpha\beta} + 2r^\alpha - \Sigma^\alpha{}_\beta r^\beta - 3A_\beta \Sigma^{\alpha\beta} - \epsilon^{\alpha\beta\gamma} N_{\beta\delta} \Sigma_\gamma{}^\delta, \quad (14)$$

$$0 = C_q \equiv q - \frac{1}{3}\Sigma^{\alpha\beta}\Sigma_{\alpha\beta} + \frac{1}{3}\boldsymbol{\partial}_\alpha r^\alpha - \frac{2}{3}A_\alpha r^\alpha, \quad (15)$$

$$0 = (C_J)^\alpha \equiv (\boldsymbol{\partial}_\beta - r_\beta)(N^{\alpha\beta} + \epsilon^{\alpha\beta\gamma}A_\gamma) - 2A_\beta N^{\alpha\beta}, \quad (16)$$

and

$$0 = (C_W)^\alpha \equiv [\epsilon^{\alpha\beta\gamma}(\boldsymbol{\partial}_\beta - A_\beta) - N^{\alpha\gamma}]r_\gamma. \quad (17)$$

We want a class of initial data satisfying these constraints that is general enough for our purposes but simple enough to find numerically. We use the York method [7] and choose H to be constant, r^α and $N_{\alpha\beta}$ to vanish, and the following form for the other variables: $E_\alpha{}^i = (\psi^{-2}/H)\delta_\alpha{}^i$, $A_\alpha = -2\psi^{-1}\boldsymbol{\partial}_\alpha\psi$, and $\Sigma_{\alpha\beta} = \psi^{-6}\mathrm{diag}(\bar\Sigma_1, \bar\Sigma_2, \bar\Sigma_3)$. Then the constraints are satisfied provided $\partial^i\bar\Sigma_i = 0$ and $q = \frac{1}{3}\psi^{-12}\bar\Sigma^i\bar\Sigma_i$ and

$$\partial^i\partial_i\psi = \frac{1}{8}H^2(6\psi^5 - \bar\Sigma^i\bar\Sigma_i\psi^{-7}). \quad (18)$$

We use the following solution for $\bar\Sigma_i$

$$\begin{aligned} \bar\Sigma_1 &= a_2\cos y + a_3\cos z + b_2 + b_3, \\ \bar\Sigma_2 &= a_1\cos x - a_3\cos z + b_1 - b_3, \\ \text{and}\quad \bar\Sigma_3 &= -a_1\cos x - a_2\cos y - b_1 - b_2 \end{aligned} \quad (19)$$

where the a_i and b_i are constants. We consider spacetimes with topology $T^3 \times R$ with each spatial slice having topology T^3. In terms of the coordinates we have $0 \le x \le 2\pi$ with 0 and 2π identified (and correspondingly for y and z).

The numerical method used is as follows: each spatial direction corresponds to $n + 2$ grid points with spacing $dx = 2\pi/n$. The variables on grid points 2 to $n + 1$ are evolved using the evolution equations, while at points 1 and $n + 2$ periodic boundary conditions are imposed. The initial data is determined once Eq. (18) is solved. This is done using the conjugate gradient method. [8] The evolution proceeds using Eqs. (4)–(9) with the exception that the term $(5 - 2q)C_q$ is added to the right hand side of Eq. (9) to prevent the growth of constraint violating modes. Spatial derivatives are evaluated using centered differences, and the evolution is done using a three step iterated Crank-Nicholson method [9] (a type of predictor-corrector method). In Eq. (9) the highest spatial derivative term is $-\frac{1}{3}\boldsymbol{\partial}^\alpha\boldsymbol{\partial}_\alpha q$ which gives this equation the form of a diffusion equation. Note that diffusion equations can only be evolved in one direction in time, in this case the negative direction which corresponds to the approach to the singularity. Stability of numerical evolution of diffusion equations generally requires a time step proportional to the square of the spatial step. However, the constant of proportionality depends on the coefficient of the second spatial derivative. To ensure stability, we define $E_{\max}$ to be the maximum value of $|E_\alpha{}^i|$ (over all space and over all α and i) and then define $dt_1 \equiv -\frac{1}{4}(dx/E_{\max})^2$ and $dt_2 \equiv -\frac{1}{8}dx$. The time step dt is then chosen to be whichever of dt_1 and dt_2 has the smaller magnitude.

Before presenting numerical results, it is helpful to consider what behavior to expect as the singularity is approached (that is as $t \to -\infty$). First denote the eigenvalues of $\Sigma^\alpha{}_\beta$ by $(\Sigma_1, \Sigma_2, \Sigma_3)$. Then suppose that at sufficiently early times the time averages of $q - \Sigma_i$ are all positive. Then the time averages of the eigenvalues of $F^\alpha{}_\beta$ are all positive. Since we are evolving in the negative time direction, this should lead [through Eq. (4)] to an exponential decrease in $E_\alpha{}^i$. However, since all spatial derivatives appear in the equations through $\boldsymbol{\partial}_\alpha = E_\alpha{}^i\partial_i$ we would expect the spatial derivatives to become negligible. That is, at each spatial point the dynamics becomes that of a spatially homogeneous cosmology: the approach to the singularity is local. Note that this does not mean that the spacetime is becoming homogeneous. Spatial variation is not becoming small; however since all spatial derivatives appear in the evolution equations through $E_\alpha{}^i\partial_i$ and since $E_\alpha{}^i$ is becoming small, the effect of the spatial derivatives on the evolution is becoming negligible. The positivity of the time averages of the eigenvalues of $F^\alpha{}_\beta$ should also lead [through Eqs. (5) and (6)] to exponential decrease in r_α and A^α. Thus we expect that as the singularity is approached, the dynamics is described by a much simpler version of evolution Eqs. (4)–(9) and constraint Eqs. (12)–(17) where r_α and A^α and all spatial derivatives are dropped.

This simpler set of equations describes homogeneous cosmologies, and has been treated extensively in the literature on such spacetimes. [5,10] Here we simply summarize the important attributes. First, from Eq. (14) it follows that $\Sigma^\alpha{}_\beta$ and $N^\alpha{}_\beta$ commute and therefore have a common basis of eigenvectors. From Eqs. (7) and (8) it follows that this basis (which we will call the asymptotic frame) is not changed under time evolution. One can therefore express Eqs. (7) and (8) in the asymptotic frame yielding equations for the Σ_i (eigenvalues of $\Sigma^\alpha{}_\beta$) and the N_i (eigenvalues of $N^\alpha{}_\beta$). During a time period where all the N_i are negligible, it follows that all the Σ_i are constant. Such a time period is called a Kasner epoch. During a Kasner epoch, two of the N_i are decaying and one is growing. The growing eigenvalue of $N^\alpha{}_\beta$ eventually gives rise to a transition (called a "bounce") to another Kasner epoch. It is helpful to define a quantity u by

$$\Sigma^\alpha{}_\beta\Sigma^\beta{}_\gamma\Sigma^\gamma{}_\alpha = 6 - \frac{81u^2(1+u)^2}{(1+u+u^2)^3} \quad (20)$$

(there is a unique $u \ge 1$ provided the quantity on the left hand side of the equation is between -6 and 6). The quantity u is constant in each Kasner epoch and changes

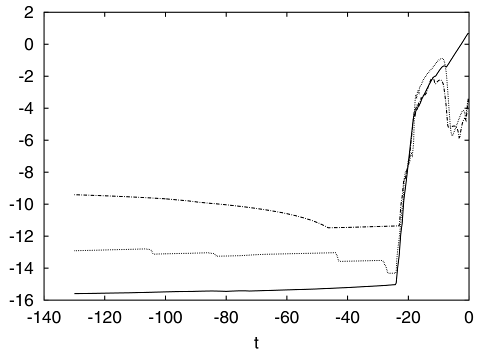

FIG. 1. Maximum values of $\ln|E_\alpha{}^i|$ (solid line), $\ln|r_\alpha|$ (dotted line) and $\ln|A^\alpha|$ (dot-dashed line) vs time.

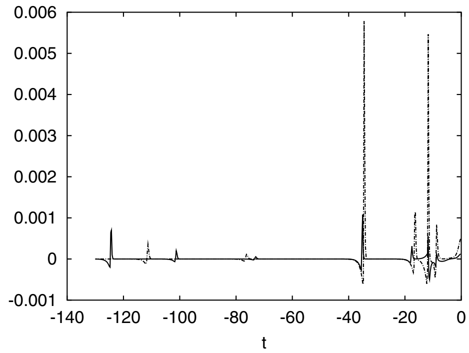

FIG. 2. Constraint C_q vs time, for $n = 50$ (solid line) and $n = 25$ (dot-dashed line).

from epoch to epoch as follows: $u \rightarrow u - 1$ if $u \geq 2$ and $u \rightarrow 1/(u - 1)$ if $1 < u \leq 2$. This rule is called the u map.

We now turn to the numerical simulations. All runs were done in double precision on a SunBlade 2000 with $n = 50$ (except for an examination of resolution which also used $n = 25$). The equations were evolved from $t = 0$ to $t = -130$. The initial value of H was $\frac{1}{3}$ corresponding to an initial trace of extrinsic curvature equal to -1. The b_i were chosen with $b_3 = 0$ and b_1 and b_2 given so that the spacetime would be a Kasner spacetime with $u = 2.3$ if the a_i vanished. For the runs presented here the a_i were given as $(0.2, 0.1, 0.04)$.

We would like to know whether $E_\alpha{}^i$, r_α, and A^α become negligible as the singularity is approached. In Fig. 1 the maximum values (over all space, α and i) of $\ln|E_\alpha{}^i|$, $\ln|r_\alpha|$, and $\ln|A^\alpha|$ are plotted as functions of time. Note the steep decrease in these quantities near $t \sim -20$. This indicates that r_α, A^α, and the spatial derivatives become negligible for $t \lesssim -20$. (The failure of the quantities plotted in Fig. 1 to continue to decrease is most likely due to unresolved small scale spatial structure to be discussed below.) Thus the interesting part of the dynamics can be seen by looking at the development of the variables at a single point as a function of time. We now present data of that form. The behavior at the spatial point chosen is typical.

The behavior of a constraint is presented in Fig. 2. Here what is plotted is C_q at the spatial point as a function of time. The solid line is for the $n = 50$ run and the dot-dashed line is for the $n = 25$ run. The finer resolution yields a smaller value for the constraint; but the resolution is not good enough to be in the convergent regime. Note that the time dependence of the two runs becomes increasingly out of sync. This is due to the chaotic nature of homogenous cosmologies. [2] Also note that the shape of the constraint for the two runs does not completely match. This may be due to unresolved small scale structure to be discussed below. Similar results were obtained for the other constraints.

Figs. 3 and 4 show, respectively, the diagonal components of $\Sigma_{\alpha\beta}$ and $N_{\alpha\beta}$ in the asymptotic frame. Though not shown here, I have also examined the off-diagonal components of both $\Sigma_{\alpha\beta}$ and $N_{\alpha\beta}$ in this frame. For times $t \lesssim -20$ these off-diagonal components become negligible. This demonstrates that for these times the asymptotic frame is essentially unchanged and the quantities in Figs. 3 and 4 are eigenvalues of $\Sigma^\alpha{}_\beta$ and $N^\alpha{}_\beta$ respectively. Note that for $t \lesssim -20$ the behavior of the components of $\Sigma_{\alpha\beta}$ consists of epochs where they are constant punctuated by short bounces where they change rapidly. Note too that for $t \lesssim -20$ the behavior of the components of $N_{\alpha\beta}$ is that they are negligible during the epochs of constant $\Sigma_{\alpha\beta}$ and that one component of $N_{\alpha\beta}$ becomes non-negligible at each bounce. This is exactly what we would expect from the approximation of using the equations for homogeneous spacetimes.

We now turn to the behavior of the quantity u. In Fig. 5 u is plotted as a function of time. Note that u undergoes a series of bounces when the components of $\Sigma_{\alpha\beta}$ do. The sequence of values of u begining at $t \sim -20$ is 1.279, 3.583, 2.584, 1.584, 1.712. This sequence obeys the u map.

In summary, these simulations provide strong support for the BKL conjecture. The initial data that are evolved have no symmetry and can be regarded as generic. The evolution shows that spatial derivatives become negligible and the time dependence goes over to the well studied behavior of a general homogeneous cosmology. This dy-

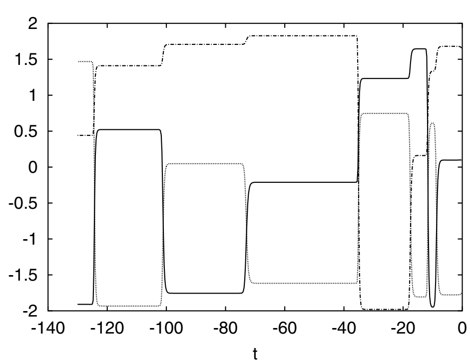

FIG. 3. Components of $\Sigma_{\alpha\beta}$ vs time, in the asymptotic frame: Σ_1 (solid line), Σ_2 (dotted line) and Σ_3 (dot-dashed line).

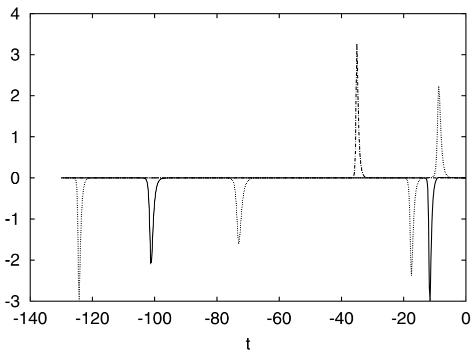

FIG. 4. Components of $N_{\alpha\beta}$ vs time, in the asymptotic frame: N_1 (solid line), N_2 (dotted line) and N_3 (dot-dashed line).

namics is oscillatory consisting of a series of Kasner epochs punctuated by short bounces. The details of the oscillations given by the behavior of the quantity u are in agreement with what would be expected for locally homogeneous spacetimes.

We now consider what remains to be done on this subject. First recall that bounces occur when one of the N_i grows exponentially. If that N_i initially vanishes on a surface S then we would expect bounces on either side of S, but not on S itself. This gives rise to a small scale structure which can be seen (crudely) in the results of these simulations, and which has been well studied in the Gowdy spacetimes. [11,12] A corresponding study for the case of no symmetry will require high resolution and is work in progress.

The present work only treats vacuum spacetimes. There is a general expectation that for most types of matter (a scalar field is an exception) the influence of the matter on the dynamics should become negligible as the singularity is approached. The formalism of reference [6] is for a fluid with equation of state $P = k\rho$ for constant k. Thus a fairly straightforward generalization of the simulations reported here would be to do simulations of the approach to the singularity for $P = k\rho$ perfect fluid.

Another question is whether there are any residual effects of the spatial derivatives as the singularity is approached. Comparison of the full evolution to one where the spatial derivatives are set to zero after a time t_0 yields differences: the sequence of bounces is the same, but they occur more rapidly in the full evolution. This may be due to the spatial derivatives' increasing the values of the N_i and thus hastening the time when the N_i become large enough to cause a bounce.

Finally, note that this simulation is for a spatially closed universe. Since the result is that the dynamics become local as the singularity is approached, these results should describe at least a portion of the singularity in any generic spacetime, including asymptotically flat spacetimes that undergo gravitational collapse to form black holes. Nonetheless, there is a body of work [13,14] that indicates that when a black hole forms, that portion of the singularity that is near the event horizon is null (or asymptotically null). It would be good to extend the methods presented here so that they are able to treat collapse in asymptotically flat spacetimes and the near horizon properties of the singularities formed.

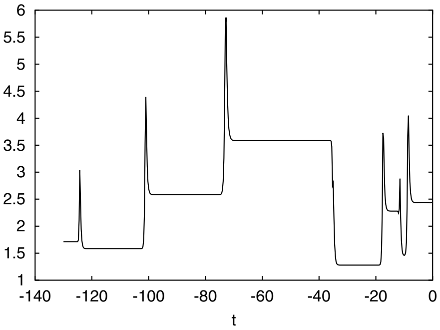

FIG. 5. u vs time.

I would like to thank Mark Miller, Beverly Berger, Woei-Chet Lim, John Wainwright, Lars Andersson, Jim Isenberg and G. Comer Duncan for helpful discussions. This work was partially supported by NSF grant PHY-0244683 to Oakland University.

*Electronic address: david@physics.uoguelph.ca

[1] for a review see A. Rendall, Living Reviews in Relativity **5**, 6 (2002).
[2] for a review see B. Berger, Living Reviews in Relativity **5**, 1 (2002).
[3] L. Andersson and A. Rendall, Commun. Math. Phys. **218**, 479 (2001).
[4] D. Garfinkle, Phys. Rev. D **65**, 044029 (2002).
[5] V. Belinskii, I. Khalatnikov, and E. Lifschitz, Sov. Phys. Usp. **13**, 745 (1971).
[6] C. Uggla, H. van Elst, J. Wainwright, and G. F. R. Ellis, Phys. Rev. D **68**, 103502 (2003).
[7] J.W. York, Phys. Rev. Lett. **26**, 1656 (1971).
[8] W. Press, S. Teukolsky, W. Vetterling, and B. Flannery, *Numerical Recipes in FORTRAN* (Cambridge University Press, Cambridge, 1992), 2nd edition.
[9] M. Choptuik, in *Deterministic Chaos in General Relativity,* edited by D. Hobill, A. Burd, and A. Coley (Plenum, New York, 1994), p. 155.
[10] *Dynamical systems in cosmology*, edited by J. Wainwright and G. F. R. Ellis (Cambridge University Press, Cambridge, England, 1997.
[11] B. Berger and D. Garfinkle, Phys. Rev. D **57**, 4767 (1998).
[12] A. Rendall and M. Weaver, Classical Quantum Gravity **18**, 2959 (2001).
[13] E. Poisson and W. Israel, Phys. Rev. D **41**, 1796 (1990).
[14] A. Ori and E. Flanagan, Phys. Rev. D **53**, 1754 (1996).

 161101-4